공초점 레이저 주사 현미경을 이용한 단섬유 복합재료 사출 성형물 내의 섬유 배열 측정 및 수치모사

이광석* • 이석원 • 윤재륜

Fiber Orientation in Injection-Molded Short Fiber Composites with a Confocal Laser Scanning Microscope and Numerical Simulation

Kwang Seok Lee, Seok Won Lee and Jae Ryoun Youn

KEY WORDS : CONFOCAL LASER SCANNING MICROSCOPY, FIBER ORIENTATION, INJECTION MOLDING, IMAGE PROCESSING, FIBER ORIENTATION TENSOR

ABSTRACT

A Confocal Laser Scanning Microscope (CLSM) is applied to determine three-dimensional fiber orientation states in injection-molded short fiber composites. Since the CLSM optically sections the composites, more than two planes either on or below the surface of composites can be obtained. Therefore, three dimensional fiber orientation states are determined without destruction. To predict the orientation states, velocity and temperature fields are calculated by using a hybrid FEM/FDM method. The change of orientation state during packing stage is also considered by employing a compressible Hele-Shaw model. The predicted orientation states show good agreement with measured ones. However, some differences are found at the end of cavity. They may result from other effects, which are not considered in the numerical analysis.

1. Introduction

Because of good mechanical properties, easiness of manufacturing, and economical advantages, injection-molded short-fiber composites are being widely used in technical and industrial applications. During the molding process a complex flow field is generated and it causes fibers to keep moving until the polymer resin is solidified. The final fiber orientation state will be retained after solidification. Thus the fiber orientation depends highly on the detail of process conditions and affects mechanical and thermal properties of the final product such as stiffness, thermal expansion, and strength. Therefore, it is important to measure the actual fiber orientation in the real composites and to apply the measured fiber orientation to characterization of the localized properties of materials and verification of the numerically predicted fiber orientation.

In determining the orientation states in the composites, the most popular method has been the calculation of directional angles of fibers from measurement of the geometrical parameters of fiber images on the only one surface of part [1,2]. Although it is a very economical and fast method, all the angles cannot be determined completely. However, by using the CSLM [3], more than two planes below the surface can be focused so that we can remove the ambiguity in determining the angles.

In this work, three-dimensional fiber orientation tensors of the composites are determined without any trade-off by using the CLSM. Measured tensors are also compared with the numerically predicted results.

* 서울대학교 재료공학부

2. Theory

Description of fiber orientation

If fibers are assumed as rigid bodies and have the same length, orientation of the fiber can be represented by a unit vector $\boldsymbol{p}$ directed toward the particle axis, as shown in *Fig. 1*. These components of $\boldsymbol{p}$ are related to θ and ϕ,

$$\begin{aligned} p_1 &= \cos\theta \\ p_2 &= \sin\theta\cos\phi \\ p_3 &= \sin\theta\sin\phi \end{aligned} \tag{1}$$

Since the CLSM is capable of optical sectioning, images of more than two planes within the sample can be obtained. Assuming that each image of a fiber that intercepts two parallel planes is identical, the directional angles (θ, ϕ) can be determined by using center coordinates of the two images as shown in *Fig.1*.

$$\theta = \tan^{-1}\left(\frac{\Delta r}{\Delta z}\right) \qquad ,\Delta x \geq 0 \tag{2}$$

$$\theta = 180° - \tan^{-1}\left(\frac{\Delta r}{\Delta z}\right) \qquad ,\Delta x < 0 \tag{3}$$

$$\phi = \tan^{-1}\left(\frac{\Delta y}{\Delta x}\right) \tag{4}$$

where $\Delta r = \sqrt{\Delta x^2 + \Delta y^2}$ (5)

Δx and Δy are the differences between the center coordinates of two images.

$$\Delta x = x_{upper} - x_{lower} \tag{6}$$

$$\Delta y = y_{upper} - y_{lower} \tag{7}$$

Δr is the distance between the two center points and Δz is the difference between upper and lower planes.

For actual composites, discrete fiber samples are measured, so components of the orientation tensor are calculated by a summation instead of the integration, as follows:

$$a_{ij} = \frac{\sum (p_i p_j) F_n}{\sum F_n} \tag{8}$$

$$F_n = \frac{1}{\cos\theta_n} \tag{9}$$

$$F_n = L/d \qquad \text{for} \quad \theta_n = 90° \tag{10}$$

where L is the length of fiber and d is the diameter of fiber. Here, F_n represents the weighting function for the nth fiber [1]. This function is required because the fiber oriented normal to the sectioning plane is more likely to intercept the plane than the fiber oriented parallel to the plane. F_n also represents the projected height of fiber onto the axis normal to the plane. The tensor has the following properties [4].

$$a_{ij} = a_{ji} \tag{11}$$

$$a_{ii} = 1 \tag{12}$$

Thus, in the second order tensor, only five of the nine components are independent.

Principles of Confocal Laser Scanning Microscopy

Simplified optics of the CLSM [5] is shown schematically in *Fig. 2*. The role of the confocal aperture is to remove out-of-focus light. As the size of the aperture is decreased, the regional image of the focal plane becomes thinner. A focal plane may be placed on the sample surface or within the sample by moving the height of objective.

3. Experimental

Process conditions for injection molding

The tensile specimens of polystyrene reinforced with 3 vol% (4.5 wt%) carbon fibers were injection-molded. The injection pressure was 8 Mpa, holding pressure was 7.5 Mpa, barrel temperature was 200°C, mold temperature was 60°C; and filling time was 1.6 sec, holding time was 5 sec, and cooling time was 25 sec.

Sample preparation, optical sectioning with the CLSM and image processing

Each sample, prepared from the specimen, was polished by using metallographic method. Specific locations of the points are described in *Fig. 3*. Two cross-sections separated by 10μm at one point were acquired by using the CLSM, Bio-Rad Radian 2000MP (NA 0.75, objective ×40, eyepiece ×10, transmission mode). The actual size of observed domain was 187 μm × 187 μm. The original micrographs obtained by the CLSM are shown in *Fig. 4*.

Two cross-sections were first enhanced by controlling the contrast and brightness and then transformed into binary images by the thresholding method in order to discard unnecessary images such as dusts and cracks. *Fig. 5* shows the examples of images after thresholding process. From given fiber images of the two sections, geometric parameters were measured. The two direction angles (θ, ϕ) of fibers were calculated from the difference between the center coordinates of the upper and lower planes, which is related with Eqn. (2) to (7). Then, the orientation tensors are determined from Eqn. (8) to (12).

4. Numerical analysis

In the analysis, flow inside the cavity is assumed to be quasi-steady, creeping, non-isothermal and inelastic. Non-Newtonian viscosity is described by the modified Cross model. Tait state equation is employed to predict the change of density with respect to pressure and temperature. Fiber orientation is predicted by solving the

evolution equation for the second order orientation tensor. The details about numerical methods are summarized in Table 1 [6].

5. Results & Discussion

Figure 6 shows that the predicted diagonal components of orientation tensors along the points 'a' through position 1 to 5 defined in *Fig. 3*. The predicted components of tensor are in good agreement with the measured ones. It can be also found that the signs of the off-diagonal components are changing along the flow direction. In *Fig. 7*, while the degree of alignment of fibers in the flow direction is slightly varying in the measured results, the predicted orientation is maintained along the points 'd' through position1 to 5 defined in *Fig. 3*. In general, the predicted orientation states correspond to the measured ones, but show some disagreement at the gate and the end of cavity. It is believed that the discrepancy is resulted from the effect of fountain flow that we did not consider in the numerical analysis, and also the initial condition may affect the predicted orientation state especially near the gate.

6. Conclusions

The use of CLSM makes it possible to remove the ambiguity in determining the off-diagonal components of tensors. By measuring the proper sign of the components, the accurate orientation states can be obtained in even complex geometry. The measured orientation states can be utilized to verify the numerical codes. Once the codes are verified, it is believed that numerical prediction can be used for the optimum design of the mold and the final product

Acknowledgements

This study was supported by the Korea Science and Engineering Foundation (KOSEF) through the Applied Rheology Center (ARC) at Korea University.

References

(1) R. S. Bay and C. L. Tucker III, *Polym Eng Sci*, (1992) 32, 240-253.
(2) P. J. Hine, N. Davidson, R. A. Duckett, A. R. Clarke and I. M. Ward, *Polym Comp*, (1996) 17, 720-729.
(3) J. L. Thomason and A. Knoester, *J Mater Sci Lett*, (1990) 9, 258-262.
(4) S. G. Advani and C. L. Tucker III, *J Rheol*, (1987) 31, 751-784.
(5) A. R. Clarke, G. Archenhold and N. C. Davidson, *Comp Sci and Tech*, (1995) 55, 75-91.
(6) S. W Lee and J. R. Youn, *Macromol Symp*, (1999) 148, 211-227.

Table 1. Methods and conditions employed for numerical analysis.

Pressure/Temperature	Hybrid FEM/FDM
Melt front advancement	Control volume method
Injection pressure	8 MPa
Holding pressure	7.5 MPa
Filling time	1.6 sec
Inlet temperature	200°C
Wall temperature	60°C
C_I	0.01
Inlet fiber orientation	Random state

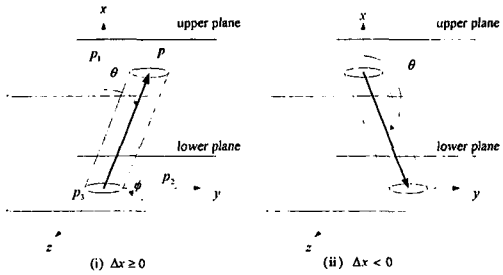

Fig. 1 The coordinate system employed to define directional angles.

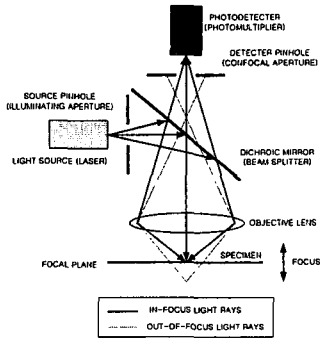

Fig. 2 Simplified optics of a confocal laser scanning microscopy.

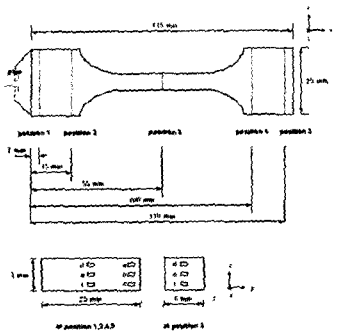

Fig. 3 Dimensions of the specimen, sampling positions and observed locations.

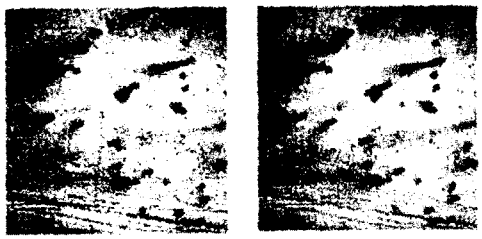

(a) upper sectioning plane. (b) lower sectioning plane.

Fig. 4 Typical micrographs taken by the CLSM.

(a) upper sectioning plane. (b) lower sectioning plane.

Fig. 5 Typical images after thresholding.

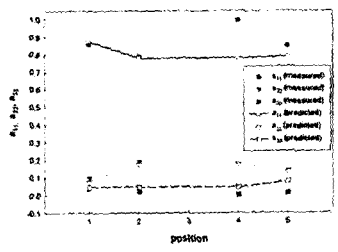

(a)

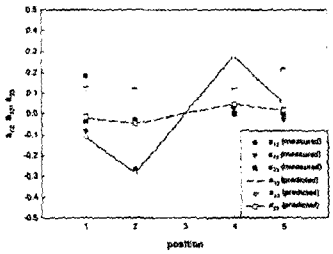

(b)

Fig. 6 Measured and predicted orientation tensors along the location 'a'; (a) diagonal terms, (b) off-diagonal terms.

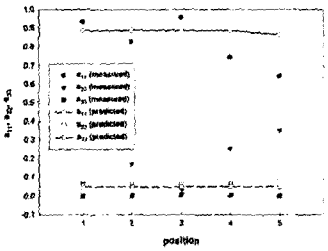

(a)

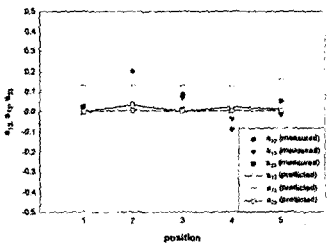

(b)

Fig. 7 Measured and predicted orientation tensors along the location 'd'; (a) diagonal terms, (b) off-diagonal terms.